

Supporting Information

Joule-Heating Synthesis of High-Entropy Oxides as Efficient Catalysts for Electrochemical Methanol Oxidation

Jiqiang Ding^{1,2}, Obeylaw Moyo², Kai Jia², Jiaqiao Yang², Zhiwei Wei², Mujia Sun²,
Bing Xue¹, Junxiong Zhang³, Na Liu^{1,*}, Hainan Sun^{2,*}

¹ Jiangsu Key Laboratory of Advanced Catalytic Materials and Technology, School of Petrochemical Engineering, Changzhou University, Changzhou, 213164, China

² School of Chemistry and Chemical Engineering, Nantong University, Nantong, 226019, China

³ School of Textile and Clothing, Nantong University, Nantong, 226019, China

E-mail: liuna@cczu.edu.cn (N. Liu); hainansun123919@ntu.edu.cn (H. Sun)

Experimental Procedures

Chemicals and Reagents

Manganese chloride ($\text{MnCl}_2 \cdot 4\text{H}_2\text{O}$, 99.0%), ferric chloride ($\text{FeCl}_3 \cdot 6\text{H}_2\text{O}$, ACS, $\geq 98\%$), cobalt chloride ($\text{CoCl}_2 \cdot 6\text{H}_2\text{O}$, ACS, $\geq 98\%$), nickel chloride ($\text{NiCl}_2 \cdot 6\text{H}_2\text{O}$, 99.9%), chromium nitrate ($\text{Cr}(\text{NO}_3)_3 \cdot 9\text{H}_2\text{O}$, 99%), potassium hydroxide (KOH, ACS, $\geq 98\%$) and methanol (CH_3OH , ACS, $\geq 99.9\%$) were purchased from Aladdin Chemistry Co., Ltd. (Beijing, China).

Joule-Heating Synthesis of High-Entropy Oxides

MnFeCoNiCr 1600K electrocatalysts were synthesized by a rapid Joule-heating method. Initially, commercial carbon felt was cut into pieces of $3 \times 2 \text{ cm}^2$, which was firstly washed by ethanol and water under the assistance of ultrasonication for 15 min, respectively. Then, the cleaned CF was thermally treated by the passage of electrical current in air condition, which could create defects on the surface of CF and improve its hydrophilicity. The optimal condition for activation step is 30 V, 40 A, 3 s. For the preparation of metal salt precursor solution, 0.1 M $\text{MnCl}_2 \cdot 4\text{H}_2\text{O}$, 0.1 M $\text{FeCl}_3 \cdot 6\text{H}_2\text{O}$, 0.1 M $\text{CoCl}_2 \cdot 6\text{H}_2\text{O}$, 0.1 M $\text{NiCl}_2 \cdot 6\text{H}_2\text{O}$, and 0.1 M $\text{Cr}(\text{NO}_3)_3 \cdot 9\text{H}_2\text{O}$ were mixed in 10 mL of water and sonicated for 10 min. After soaking the activated CF in the precursor solution for 10 min, it was placed in an oven at $80 \text{ }^\circ\text{C}$ to dry overnight. Then the above heat treatment steps were repeated for the CF coated with dried precursors, and the optimal condition is 30 V, 60 A, 1600 K. The obtained MnFeCoNiCr 1600K was washed with deionized water and dried for electrochemical testing. Joule heating was performed using a HTS-3016D ultrafast heating system (Shenzhen Zhongke Jingyan Technology Co., Ltd., China). Other control catalysts were synthesized following a similar procedure, with variations only in the types of metal precursors and the heating temperatures.

Physical Characterizations

X-ray diffraction (XRD) patterns were collected on a Rigaku D8 diffractometer. The morphology of the catalysts was characterized using scanning electron microscopy (SEM, JEOL JSM-6700F) and transmission electron microscopy (TEM, JEOL ARM-200FTH). High-resolution X-ray photoelectron spectroscopy (XPS) measurements were conducted on the Thermo Scientific Escalab 250 Xi under ultra-high vacuum conditions ($< 10^{-6}$ bar). Liquid products of the MOR were characterized via ^1H nuclear magnetic resonance (NMR, Bruker) spectroscopy.

Electrochemical Measurements

All electrochemical measurements were conducted in a standard three-electrode configuration using a CS2350M bipotentiostat (Corrtest, Wuhan, China). The as-prepared self-supported catalysts were directly used as the working electrodes, with a graphite rod and an Hg/HgO electrode serving as the counter and reference electrodes, respectively. The electrolyte for methanol oxidation consisted of 1.0 M KOH containing 1.0 M methanol. Linear sweep voltammetry (LSV) measurements were performed at a scan rate of 5 mV s^{-1} . Unless otherwise specified, all potentials were converted to the reversible hydrogen electrode (RHE) scale and corrected for iR compensation according to $E_{\text{RHE}} = E_{\text{Hg/HgO}} + 0.925 - iR$, where i is the current and R is the internal resistance obtained from electrochemical impedance spectroscopy (EIS).

Operando Raman Spectroscopy

Operando Raman was conducted using a three-electrode Raman cell was used for the measurements. The applied potential was maintained for 90 s before each measurement to ensure its equilibrium state. For the measurements, 1 M KOH and 1 M ethanol was used as the electrolyte. The acquisition time was set to 5 s, and complete spectra were acquired by averaging 10 scans.

Differential Electrochemical Mass Spectrometry (DEMS)

DEMS (QAS100, Shanghai Linglu Instrument) combined with an electrochemical workstation (Corrtest, Wuhan, China) was employed in a typical three-electrode electrochemical cell. 1 M KOH with 1 M methanol was used as the electrolyte. The

working electrode was paved on a porous PTFE membrane, where the hydrophobic PTFE membrane permits gas flow while rejecting liquid. To trap the water vapour for averting potential damages to the mass spectrometer, a cold trap cooled with dry ice was installed between the electrochemical cell and the vacuum chamber. CV scan was conducted with a scan rate of 5 mV s^{-1} over a potential range of 1.0 to 1.45 V vs. RHE, while recording the mass signals m/z of different volatile products.

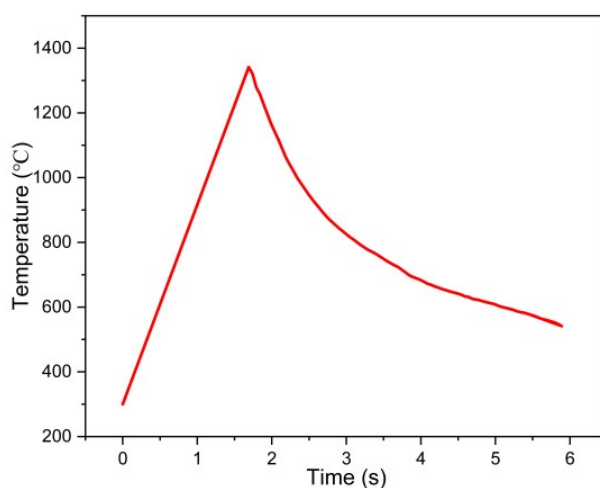


Fig. S1. Joule-heating process for MnFeCoNiCr-1600 K synthesis. Temperature-time profile showing ultrafast heating ($\sim 1600 \text{ K}$) and rapid cooling during nanoparticle formation.

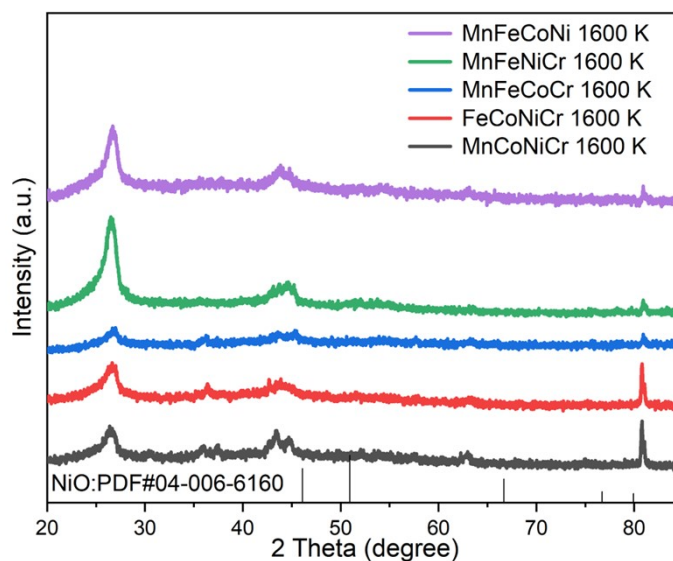


Fig. S2. XRD patterns of MnFeCoNiCr-1600 K, MnFeCoNiCr-1300 K, FeCoNiCr-1600 K, MnFeCoCr-1600 K, MnFeCoNi-1600 K, and MnFeNiCr-1600 K, confirming the formation of a rock-salt-type phase.

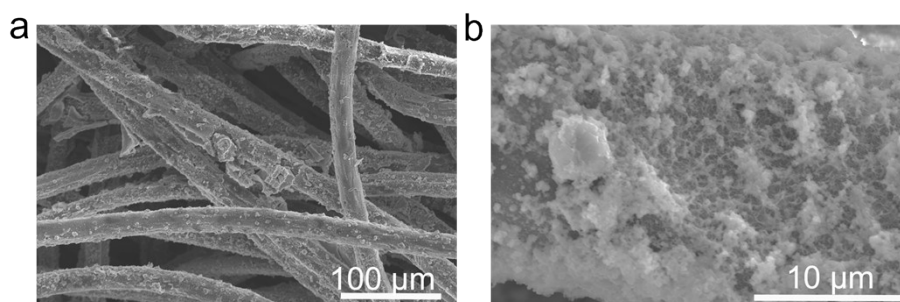


Fig. S3. SEM images of MnFeCoNiCr-1600K with different magnifications.

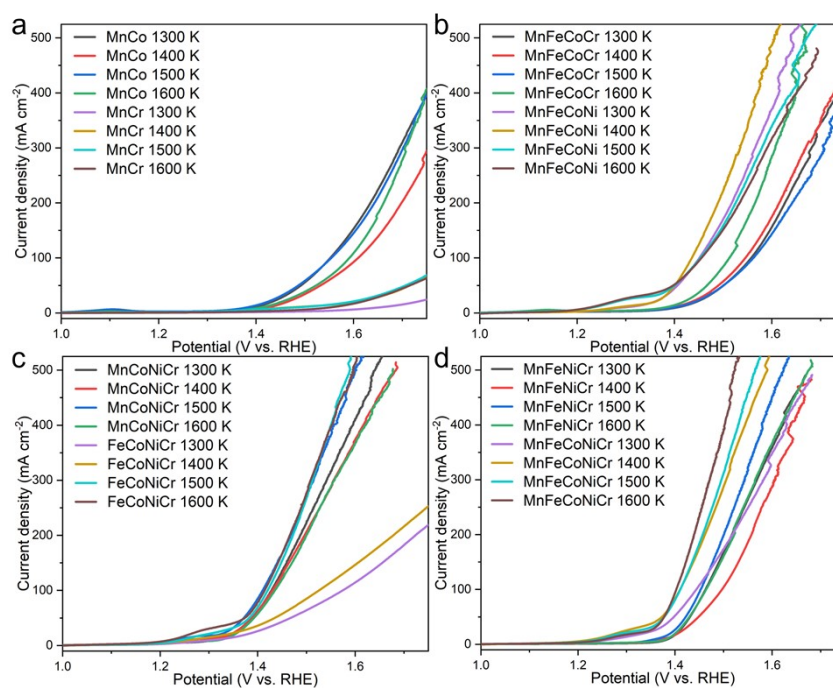


Fig. S4. LSV curves of additional catalysts synthesized at different compositions and temperature for methanol oxidation in 1 M KOH with 1 M methanol.

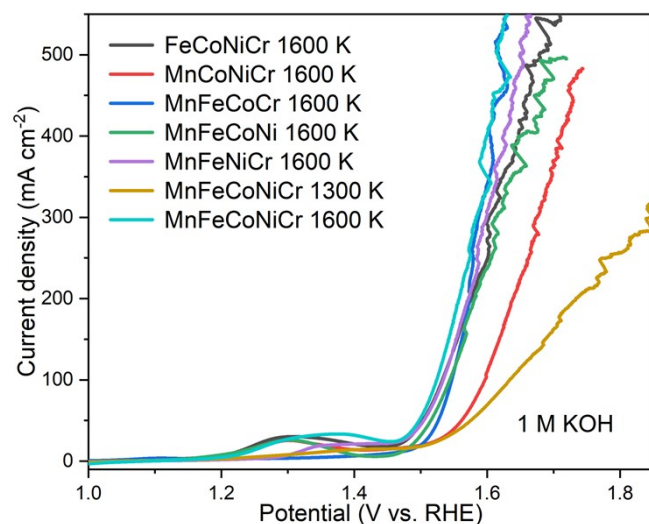


Fig. S5. OER polarization curves of all investigated catalysts in 1 M KOH.

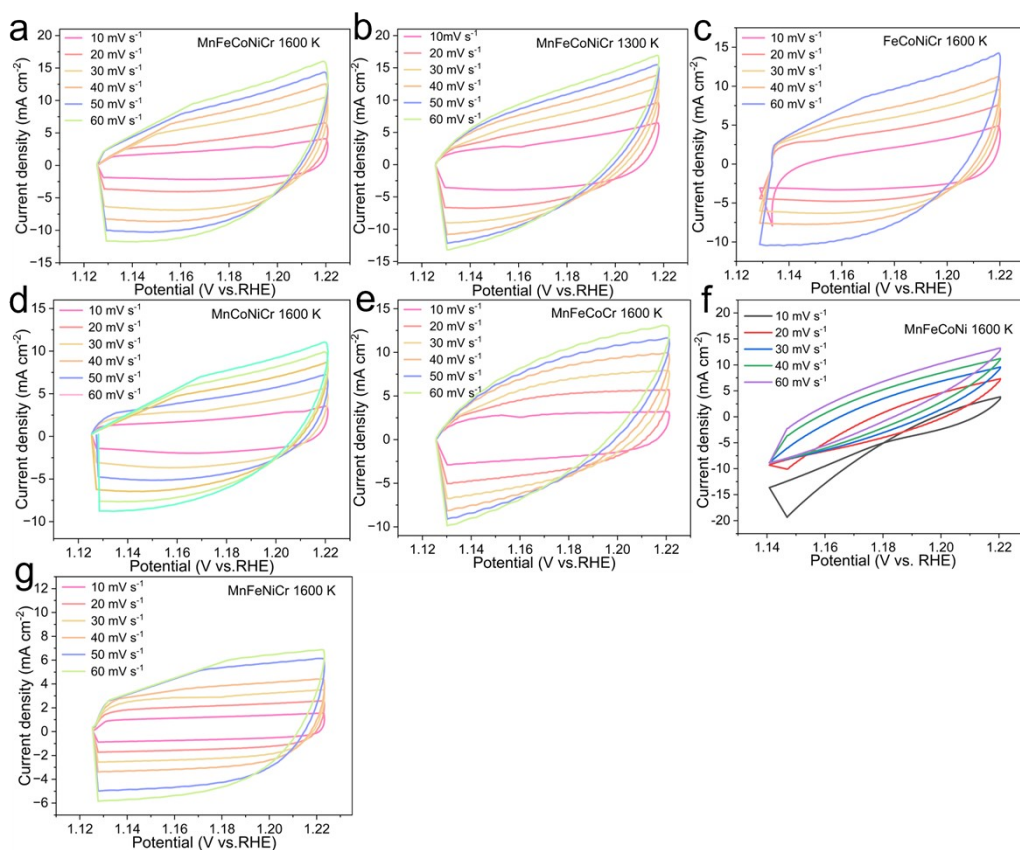


Fig. S6. CV curves of studied electrocatalysts.

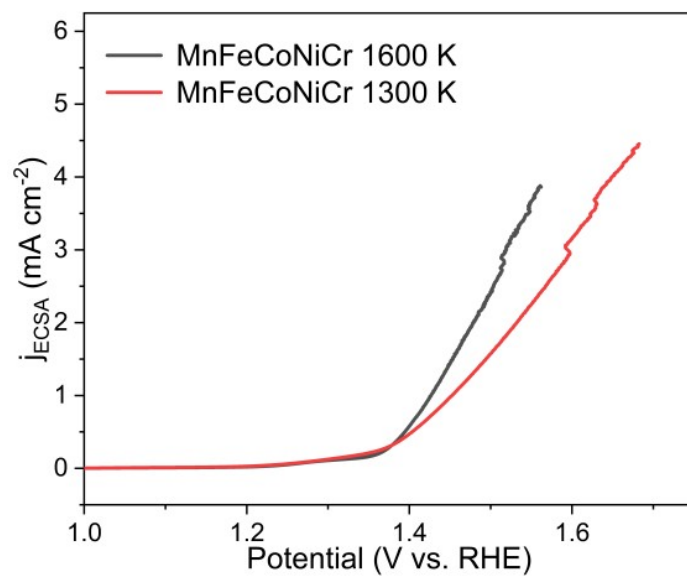


Fig. S7. ECSA-normalized catalytic activities of MnFeCoNiCr 1600K and 1300K.

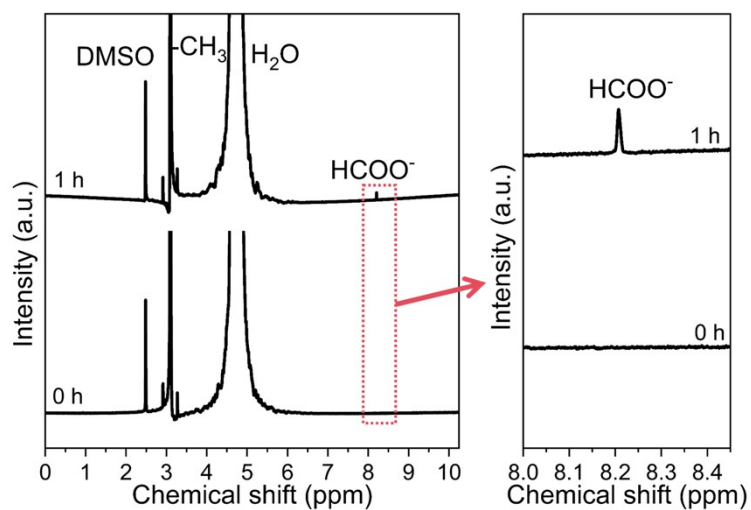


Fig. S8. ^1H NMR spectra of liquid products before and after testing.

Tab. S1. Comparison of methanol oxidation performance of MnFeCoNiCr-1600K and MnFeCoNiCr-1300K with others previously reported catalysts at current densities of 50 and 100 mA cm⁻².

Catalyst	Electrolyte	Potential (V vs. RHE) @ 50 mA cm ⁻²	Potential (V vs. RHE) @ 100 mA cm ⁻²	Ref.
Ni-Mo ₂ C@C	1 M KOH + 1 M methanol	1.43	1.49	[1]
NiCo	1 M KOH + 1 M methanol	1.43	1.53	[2]
Si-Co(OH) ₂ /NF	1 M KOH + 1 M methanol	1.37	1.41	[3]
Ni50Co50-m	1 M KOH + 1 M methanol	1.45	1.51	[4]
(HEO) ₂ /Max ₁	1 M KOH + 1 M methanol	1.45	1.53	[5]
F ₁₀ -Ni ₃ N	1 M KOH + 1 M methanol	1.38	1.43	[6]
Ni/MoN	1 M KOH + 0.5 M methanol	1.40	1.48	[7]
Co/SiO ₂	1 M KOH + 1 M methanol	1.44	1.49	[8]
CNFs@NiSe/CC	1 M KOH + 1 M methanol	1.38	1.43	[9]
Cr _{0.02} Ni(OH) _{2+δ}	1 M KOH + 1 M methanol	1.45	1.50	[10]
MnFeCoNiCr 1300K	1 M KOH + 1 M methanol	1.40	1.44	This work
MnFeCoNiCr 1600K	1 M KOH + 1 M methanol	1.38	1.40	This work

References:

- [1] Lin G, Qin H, Cao X, et al. Regulation of Relay Catalytic Mechanism for Efficient Methanol Oxidation Reaction. *Angew. Chem. Int. Ed.* 2025, 137(42): e202506215.
- [2] Zheng Z, Zheng X, Wang L, et al. Harnessing Electrocatalytic Coupling of Carbon Dioxide and Methanol for High-Efficiency Formic Acid Production. *Angew. Chem. Int. Ed.* 2025, 64(43): e202512078.
- [3] Pu J, Xie B, Sun Y, et al. Interfacial microenvironment engineering triggered by rapid silicon doping for promoted methanol electrooxidation. *Appl. Surface Sci.* 2026, 729: 166279.
- [4] Qi Y, Zhu Y, Jiang H, et al. Promoting electrocatalytic oxidation of methanol to formate through interfacial interaction in NiMo oxide-CoMo oxide mixture-derived catalysts. *Chinese J. Catal.* 2024, 56: 139-149.
- [5] He H, Xu C, Jiang Q, et al. High-Entropy Spinel Oxides-Decorated MXene Nanoarchitectures for Efficient Methanol Oxidation-Assisted Hydrogen Production. *Small*, 2026: e14116.
- [6] Qin H, Li J, Lin G, et al. Tuning surface coordination environment of Ni₃N by fluorine modification for efficient methanol electrooxidation assisted hydrogen evolution. *Adv. Mater.* 2025, 37(33): 2507573.
- [7] Rao C, Wang H, Chen K, et al. Hybrid acid/base electrolytic cell for hydrogen generation and methanol conversion implemented by bifunctional Ni/MoN nanorod electrocatalyst. *Small* 2024, 20(7): 2303300.
- [8] Jing S, Wang G, Li Z, et al. Maintaining local alkalinity of CO-electroreduction full cell by silica-confined electrocatalysts in membrane electrode assembly. *Sci. Adv.* 2025, 11(48): eacb3478.
- [9] Zhao B, Liu J W, Yin Y R, et al. Carbon nanofibers@NiSe core/sheath nanostructures as efficient electrocatalysts for integrating highly selective methanol conversion and less-energy intensive hydrogen production. *J. Mater. Chem. A*, 2019, 7(45): 25878-25886.
- [10] Qin H, Ye Y, Lin G, et al. Regulating the electrochemical microenvironment of

Ni (OH)₂ by Cr doping for highly efficient methanol electrooxidation. ACS Catal. 2024, 14(21): 16234-16244.